Robust Time-Delayed PID Flight Control for Automatic Landing Guidance under Actuator Loss-Of-Control

Balaji Jayaraman[1] * **Vikram Kumar Saini**[2] *
Ajoy Kanti Ghosh[3] *

* *Department of Aerospace Engineering, Indian Institute of Technology Kanpur, Uttar Pradesh - 208016, INDIA.*

Abstract: A robust fault-tolerant flight control scheme for aircraft attitude tracking for longitudinal automatic landing guidance under actuator loss-of-control using a Time-Delayed PID control law is presented in this work. Since the formulation of controllers involving time-delay are similar to incremental nonlinear dynamic inversion, these control schemes are independent of model knowledge and therefore robust to unfavourable variations in the system parameters. This property of the time-delay controller is used to develop a discrete-time PID control law that can alleviate the effects of multiple actuator faults during landing phase of a fixed-wing aircraft.

Keywords: Fault-Tolerant Flight Control, Time-Delay Control, Discrete-Time PID Control, Incremental Nonlinear Dynamic Inversion, Actuator Loss-Of-Control.

1. INTRODUCTION

Fault-Tolerant Flight Control (FTFC) systems are characterised by the ability to endure loss-of-control events, while demonstrating a desirable flight performance and maintaining the stability characteristics of the aircraft (Lombaerts et al. (2011); Zhang and Jiang (2008)). While active FTFC systems are characterised by a fault-detection and diagnosis mechanism and a reconfiguration mechanism for control action, passive systems are simply designed to be robust to system faults in general.

Baseline feedback linearization approaches like Incremental Nonlinear Dynamic Inversion (INDI) (Sieberling et al. (2010); Acquatella et al. (2012); Simplício et al. (2013); Smeur et al. (2016)) and Time-Delay Control (TDC) (Youcef-Toumi and Wu (1992); Marquez-Martinez and Moog (2004); Roy et al. (2017a,b)) have been proved to be robust to component faults due to the robustness in formulation, predominantly for uncertain nonlinear systems with an aim to reduce dependency on explicit system modeling. While INDI has been extensively used in control of aerospace vehicles, TDC is a well known approach in robot control. When realized in second-order controller canonical form, a relationship between TDC and a discrete-time PID controller can be derived, which has been useful in implementation of TDC for a wide range of dynamic systems (Jung et al. (2011); Reddy (2020a,b)). PID controllers are well known for the effectiveness in a wide spectrum of applications, especially when conceived in digital form (Chang and Jung (2008)). Owing to the equivalence of a discrete-time PID to TDC, the control gains can very well be determined by a systematic method so that it retains the robustness in performance and simplicity in implementation, which are the positive attributes of TDC (Chang and Jung (2008)) that could be demonstrated for sufficient performance under substantial system uncertainties and could simplify the gain tuning procedure.

In the context of flight control, the aircraft attitude tracking problem can be formulated in such a manner that the aircraft Euler attitude can be mapped to the aircraft control surface deflections in second-order controller canonical form. This framework has been used to develop aircraft angular rate control system for a fixed-wing aircraft by establishing an equivalence between INDI and TDC (Acquatella et al. (2017)). With prior attempts in designing a TDC for fault-tolerant control of longitudinal flight have been demonstrated in literature (Choi et al. (2010); Lee et al. (2012)), this has been extended in the present work in designing a discrete-time PID controller based on TDC, termed Time-Delayed PID (TD-PID) controller for the aircraft attitude tracking problem of the Hansa-3 aircraft. The PID gains are tuned systematically via INDI controller by defining the desired error dynamics and effector blending moments, and the controller performance has been evaluated for guidance during landing phase under loss-of-control due to successive actuator impairments. The results are compared with INDI Control and taking NDI control as a benchmark.

This paper is organised as follows. The problem formulation for landing trajectory generation and conversion of the desired landing trajectory into attitude tracking reference and actuator fault modeling is discussed in Section 2, and a theoretical framework for aircraft attitude control design using TD-PID control law is presented in Section 3. Results of closed-loop simulation performed on the Hansa-

⋆ [1,2] Ph D Candidate, Flight Mechanics and Control, balaji.j09@gmail.com
⋆⋆[3] Professor (Retd.), Flight Mechanics and Control, akg@iitk.ac.in

3 aircraft model is presented and discussed in Section 4. The conclusions are finally drawn in Section 5.

2. PROBLEM FORMULATION

2.1 Landing Profile and Attitude Reference Generation

In this subsection, the landing profile for the Hansa-3, a general aviation aircraft used in the Flight Laboratory of IIT Kanpur for experimentation purposes, is discussed.

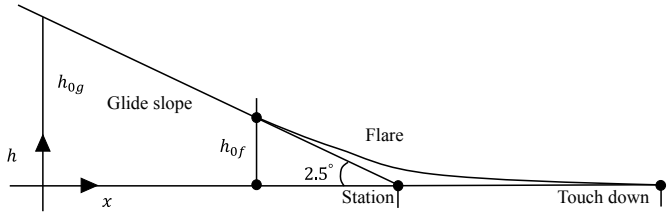

Fig. 1. Desired Landing Profile.

The aircraft landing profile generally consists of two phases: the glide phase and the flare phase, as shown in Fig. 1. The mathematical representation of the landing trajectory h_d is given by

$$h_d = \begin{cases} -tan(\theta_a)\ x + h_{0_g} & ;\ \text{(glide)} \\ h_{0_f}\ e^{-t/\varsigma} & ;\ \text{(flare)} \end{cases} \tag{1}$$

where θ_a is the approach angle, x is the forward distance, h_{0_g} and h_{0_f} are the initial glide and flare altitudes and ς is the time constant the defines the curvature of the flare phase. For the current work $\theta_a = 2.5°$, $h_{0_g} = 50m$, $h_{0_f} = 10m$ and $\varsigma = 6$ are taken. Now, in order to maintain a coordinated motion during landing, the desired landing trajectory is defined in terms of the rate of descent $\dot{h}_d$ and directional motion $\dot{y}_d$ as

$$\dot{h}_d = V_a\ sin(\gamma_d) \tag{2a}$$

$$\dot{y}_d = V_a\ cos(\theta_d)\ sin(\psi_d) \tag{2b}$$

While the desired bank angle ϕ_d is maintained at the trim condition (Table 4), the desired pitch (θ_d) and yaw (ψ_d) angles for tracking the landing profile are obtained from (2) as

$$\theta_d = \gamma_d + \alpha \tag{3a}$$

$$\psi_d = sin^{-1}\left(\frac{\dot{y}_d}{V_a\ cos(\theta_d)}\right) \tag{3b}$$

where

$$\gamma_d = sin^{-1}\left(\frac{\dot{h}_d}{V_a}\right)$$

The automatic landing guidance problem is now simplified into an attitude tracking problem, the derivation of the control law for which will be discussed in Section 3.2.

2.2 Actuator Fault Modeling

The actuator model is representative of a first-order transfer function in time-domain format.In this work, a polynomial series is considered for modeling actuator faults as shown in the below expression (Kim et al. (2003)).

$$\delta_f = b_0 + b_1\delta_c \tag{4}$$

Where b = $[b_0,\ b_1]$ is the fault coefficient vector, $b_0 = \delta_0$, a disturbance term representing actuator jamming condition, b_1 is the control effectiveness parameter. Since jammed control surfaces induce additional aerodynamic derivatives, and due to the unavailability of data corresponding to the specific faults, for the present work, only cases of partial loss of control are simulated for performance evaluation of the controller of interest.

Table 1. Actuator Fault Cases

Case	b_0	b_1
no fault	0	1
jammed/total LOC	$\in$[± position limit]	0
partial LOC	0	$\in (0, 1)$

3. FAULT TOLERANT FLIGHT CONTROL DESIGN

3.1 Flight Vehicle Modeling

The aircraft attitude dynamics can be represented in a compact form as

$$\begin{aligned} \dot{\boldsymbol{\Theta}} &= \boldsymbol{T}(\boldsymbol{\Theta})\ \boldsymbol{\Omega} \\ \dot{\boldsymbol{\Omega}} &= \boldsymbol{J}^{-1}\big[-\boldsymbol{\Omega} \times \boldsymbol{J}\boldsymbol{\Omega} + \boldsymbol{M}^b\big] \end{aligned} \tag{5}$$

where $\boldsymbol{\Theta} = [\phi,\ \theta,\ \psi]$ and $\boldsymbol{\Omega} = [p,\ q,\ r]$ are the attitude and the body rates, respectively, and $\boldsymbol{J}$ is the inertia matrix and $\boldsymbol{M}^b = [L,\ M,\ N]$ is the moment vector in body axes. While the nominal aerodynamic model of Hansa-3 is given in (Kumar and Ghosh (2018); Peyada and Ghosh (2009)), the aerodynamic moments can be written in terms of the corresponding coefficients and can be broken down into the form

$$\boldsymbol{M}^b = \boldsymbol{M}^b_A + \boldsymbol{M}^b_C\ \boldsymbol{u} \tag{6}$$

where $\boldsymbol{M}^b_A = [L_A,\ M_A,\ N_A]$ and $\boldsymbol{M}^b_C = [L_C,\ M_C,\ N_C]$, and $\boldsymbol{u} = [\delta_a,\ \delta_e,\ \delta_r]$ is the control input vector, and

$$\boldsymbol{M}^b_A = q_\infty S\ \text{diag}([b\ \bar{c}\ b]) \begin{bmatrix} C_l(\beta,\ \hat{p},\ \hat{r}) \\ C_m(\alpha,\ \hat{q}) \\ C_n((\beta,\ \hat{p},\ \hat{r}) \end{bmatrix} \tag{7a}$$

is the control independent term and

$$\boldsymbol{M}^b_C = q_\infty S\ \text{diag}([b\ \bar{c}\ b]) \begin{bmatrix} C_{l_{\delta_a}} & 0 & 0 \\ 0 & C_{m_{\delta_e}} & 0 \\ 0 & 0 & C_{n_{\delta_r}} \end{bmatrix} \tag{7b}$$

is the control dependent term, otherwise termed as the effector blending moment term, and $q_\infty = \frac{1}{2}\rho V_a^2$ is the dynamic pressure, V_a is the airspeed, S is the wing

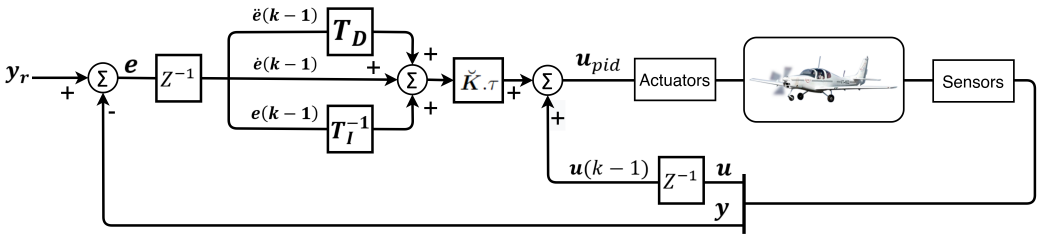

Fig. 2. Discrete-Time PID Attitude Control Framework for Hansa-3 Aircraft.

reference area, ρ is the atmospheric pressure, α is the angle of attack and β is the sideslip angle, and

$$\hat{p} = \frac{p\ b}{2\ V_a}, \quad \hat{q} = \frac{q\ \bar{c}}{2\ V_a} \quad \text{and} \quad \hat{r} = \frac{r\ b}{2\ V_a}$$

are the nondimensionalised aircraft body rates, where b is the wing span and $\bar{c}$ is the wing mean aerodynamic chord. For the design of the feedback control law, the following assumption is made for the aircraft kinematics

$$\dot{\boldsymbol{\Theta}} \approx \boldsymbol{\Omega} \tag{8}$$

Based on the above assumptions and substituting (6) in (5), the aircraft rate dynamics can now be rewritten as

$$\ddot{\boldsymbol{\Theta}} = \boldsymbol{J}^{-1}\big[-\boldsymbol{\Omega} \times \boldsymbol{J}\boldsymbol{\Omega} + \boldsymbol{M}_A^b\big] + \boldsymbol{J}^{-1}\boldsymbol{M}_C^b\ \boldsymbol{u} \tag{9}$$

which is in second-order controller canonical form and will be used in the flight control design.

3.2 Discrete-Time PID Based on Time-Delay Control

Following the aircraft attitude dynamics derived in (9), it can be represented in INDI form as

$$\ddot{\boldsymbol{y}} = \ddot{\boldsymbol{y}}_0 + \boldsymbol{J}^{-1}\bar{\boldsymbol{M}}_{C_0}^b\ (\boldsymbol{u} - \boldsymbol{u}_0) \tag{10}$$

where $\boldsymbol{y} = [\phi,\ \theta,\ \psi]$ and $\ddot{\boldsymbol{y}}_0$, $\boldsymbol{u}_0$ and $\bar{\boldsymbol{M}}_{C_0}^b$ are the state derivative, the input and the control moment matrix at previous time step, respectively. Rewriting (10) in time-delayed form as

$$\ddot{\boldsymbol{y}}(t) = \ddot{\boldsymbol{y}}(t-\tau) + \breve{\boldsymbol{\mathcal{B}}}\ \big[\boldsymbol{u}(t) - \boldsymbol{u}(t-\tau)\big] \tag{11}$$

where $\breve{\boldsymbol{\mathcal{B}}} \triangleq \bar{\boldsymbol{J}}^{-1}\bar{\boldsymbol{M}}_C^b$, and $\bar{\boldsymbol{J}}$ and $\bar{\boldsymbol{M}}_C^b$ denote the nominal values of the inertia matrix and the effector blending moments, and τ is the sampling time. Now, the discrete-time formulation of (11) can be written as

$$\ddot{\boldsymbol{y}}(k) = \ddot{\boldsymbol{y}}(k-1) + \breve{\boldsymbol{\mathcal{B}}}\ \big[\boldsymbol{u}(k) - \boldsymbol{u}(k-1)\big] \tag{12}$$

where $t = \tau k$. Now, for the attitude reference commands $\boldsymbol{y}_r = [\phi,\ \theta,\ \psi]_r$, denoting the tracking error vector as $\boldsymbol{e}(k) = \boldsymbol{y}_r(k) - \boldsymbol{y}(k)$, the TDC law in discrete-time form can be written as

$$\begin{aligned}\boldsymbol{u}(k) = \boldsymbol{u}(k-1) + \breve{\boldsymbol{\mathcal{B}}}^{-1}\big[&-\ddot{\boldsymbol{y}}(k-1) + \ddot{\boldsymbol{y}}_r(k) \\ &+ \boldsymbol{K}_D\ \dot{\boldsymbol{e}}(k) + \boldsymbol{K}_P\ \boldsymbol{e}(k)\big]\end{aligned} \tag{13}$$

Based on the causality relationship defined in (Chang and Jung (2008)), it is necessary to transform $\ddot{\boldsymbol{y}}_d(k)$, $\dot{\boldsymbol{e}}(k)$ and $\boldsymbol{e}(k)$ to $\ddot{\boldsymbol{y}}_r(k-1)$, $\boldsymbol{e}(k-1)$ and $\boldsymbol{e}(k-1)$. Now, since $\ddot{\boldsymbol{y}}_r(k-1)$ and $\ddot{\boldsymbol{y}}(k-1)$ emerge at the same sampling instant, (13) can now be rewritten as

$$\begin{aligned}\boldsymbol{u}(k) = \boldsymbol{u}(k-1) + \breve{\boldsymbol{\mathcal{B}}}^{-1}\big[&\ddot{\boldsymbol{e}}(k-1) + \boldsymbol{K}_D\ \dot{\boldsymbol{e}}(k-1) \\ &+ \boldsymbol{K}_P\ \boldsymbol{e}(k-1)\big]\end{aligned} \tag{14}$$

where $\ddot{\boldsymbol{e}}$ and $\dot{\boldsymbol{e}}$ are computed at through numerical differentiation using the following equations:

$$\begin{aligned}\dot{e}(k) &= \frac{e(k) - e(k-1)}{\tau} \\ \ddot{e}(k) &= \frac{e(k) - 2e(k-1) + e(k-2)}{\tau^2}\end{aligned} \tag{15}$$

Now, considering a standard Proportional-Integral-Derivative controller in continuous-time as

$$\boldsymbol{u}_{pid}(t) = \breve{\boldsymbol{K}}\Big[\boldsymbol{e}(t) + \boldsymbol{T}_D\ \dot{\boldsymbol{e}}(t) + \boldsymbol{T}_I^{-1}\int_0^t \boldsymbol{e}(\sigma)d\sigma\Big] + \boldsymbol{u}_{dc} \tag{16}$$

where $\breve{\boldsymbol{K}}$, $\boldsymbol{T}_D$ and $\boldsymbol{T}_I$ denote 3×3 constant diagonal matrices representing proportional gain, derivative time and integral time respectively, and $\boldsymbol{u}_{dc}$ is a 3×1 vector representing dc-bias governed by initial conditions, where in the case of aircraft, it refers to the initial trim conditions. By taking $\boldsymbol{u}_{dc} = \boldsymbol{u}(k-1)$, an equivalence between TDC and PID can be represented in discrete-time formulation as

$$\begin{aligned}\boldsymbol{u}_{pid}(k) = \breve{\boldsymbol{K}}\Big[&\boldsymbol{e}(k-1) + \boldsymbol{T}_D\ \dot{\boldsymbol{e}}(k-1) \\ &+ \boldsymbol{T}_I^{-1}\sum_{\sigma=0}^{k-1}\tau\ \boldsymbol{e}(\sigma)\Big] + \boldsymbol{u}(k-1)\end{aligned} \tag{17}$$

The equivalence of the above equation to TDC is therefore derived by obtaining $\boldsymbol{u}(k-1)$ for $k \geq 2$ and subtracting it from $\boldsymbol{u}(k)$, which transform (17) to

$$\begin{aligned}\boldsymbol{u}_{pid}(k) - \boldsymbol{u}(k-1) = \breve{\boldsymbol{K}}\big[&\boldsymbol{e}(k-1) - \boldsymbol{e}(k-2) \\ &+ \boldsymbol{T}_D\ (\dot{\boldsymbol{e}}(k-1) - \dot{\boldsymbol{e}}(k-2)) \\ &+ \boldsymbol{T}_I^{-1}\tau\ \boldsymbol{e}(k-1)\big]\end{aligned} \tag{18}$$

Further replacing the $\dot{\boldsymbol{e}}(\cdot)$ in terms of $\boldsymbol{e}(\cdot)$ by application of numerical differentiation (15) yields

$$\begin{aligned}\boldsymbol{u}_{pid}(k) =& \boldsymbol{u}(k-1) + \breve{\boldsymbol{K}}\ \tau\Bigg\{\left(\frac{\boldsymbol{e}(k-1)-\boldsymbol{e}(k-2)}{\tau}\right)\\ &+ \mathbf{T}_D\left(\frac{\boldsymbol{e}(k-1)-2\boldsymbol{e}(k-2)+\boldsymbol{e}(k-3)}{\tau^2}\right)\\ &+ \mathbf{T}_I^{-1}\boldsymbol{e}(k-1)\Bigg\}\end{aligned} \tag{19}$$

Now deriving a relationship between (14) and (19) and using (15) in (19), the discrete-time PID control law for aircraft attitude tracking in obtained as

$$\begin{aligned}\boldsymbol{u}_{pid}(k) = \boldsymbol{u}(k-1) + \breve{\boldsymbol{K}}\ \tau\Big[&\mathbf{T}_D\ \ddot{\boldsymbol{e}}(k-1)\\ &+ \dot{\boldsymbol{e}}(k-1) + \mathbf{T}_I^{-1}\ \boldsymbol{e}(k-1)\Big]\end{aligned} \tag{20}$$

The parameters of the discrete-time PID control law (20) can be obtained by drawing a comparison with (14) and obtaining the following relationships:

$$\breve{\boldsymbol{K}} = \boldsymbol{K}_D\ (\tau\ \breve{\boldsymbol{\mathcal{B}}})^{-1},\ \boldsymbol{T}_D = \boldsymbol{K}_D^{-1} \text{ and } \boldsymbol{T}_I = \boldsymbol{K}_D\ \boldsymbol{K}_P^{-1}$$

While the derivative and integral time are decided by the choice of $\boldsymbol{K}_D$ and $\boldsymbol{K}_P$, the robustness of the discrete-PID controller can be further enhanced by tuning the proportional gain $\breve{\boldsymbol{K}}$, which can be considered as a scheduled gain. By taking a diagonal elements of the nominal effector blending moment matrix $\breve{\boldsymbol{\mathcal{B}}}(\boldsymbol{x}) = \bar{\boldsymbol{J}}^{-1}\bar{\boldsymbol{M}}_C^b$ used in INDI control, the self scheduling properties of $\breve{\boldsymbol{\mathcal{B}}}(\boldsymbol{x})$ are now lost, so that $\breve{\boldsymbol{K}}$ can be tuned based on the standard method used in TDC (Chang and Jung (2008); Acquatella et al. (2017)) to achieve satisfactory closed loop performance.

4. SIMULATION AND RESULTS

The performance of the Time-Delayed PID controller in comparison with the INDI controller for automatic landing of Hansa-3 aircraft under actuator loss-of-control is evaluated numerically and the results presented in this section. Also, to demonstrate the robustness of the TD-PID controller, the results are also compared with classical NDI controller as the benchmark. The aircraft nominal equations of motion are set up with an actuator model presented in Table. 2, and a sensor noise model with a standard deviation of 10^{-3} in the accelerations, body rates, airspeed, angle of attack and sideslip measurements, and the simulation models are built in Simulink® environment.

Table 2. Actuator Specifications.

Actuators	Position Limit	Rate Limit	Bandwidth
δ_a, δ_e, δ_r	$\pm$20 deg	100 degs^{-1}	16 rads^{-1}

The simulation is initiated from the trim conditions defined in Table 3, from an initial altitude of $h = 50$ m. For fair comparisons, the second-order error model of all the controllers is defined by the controller gains $K_{D_i} = 7$ and $K_{P_i} = 25$, $i = 1, 2, 3$, for the NDI and INDI controllers. The PID rate and reset times are obtained based on the

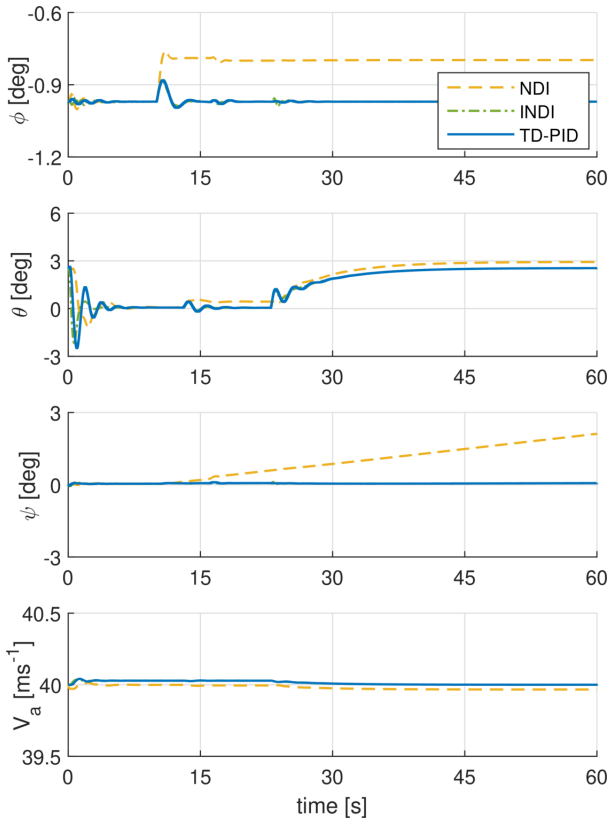

Fig. 3. Attitude and Airspeed response under 25% loss-of-control.

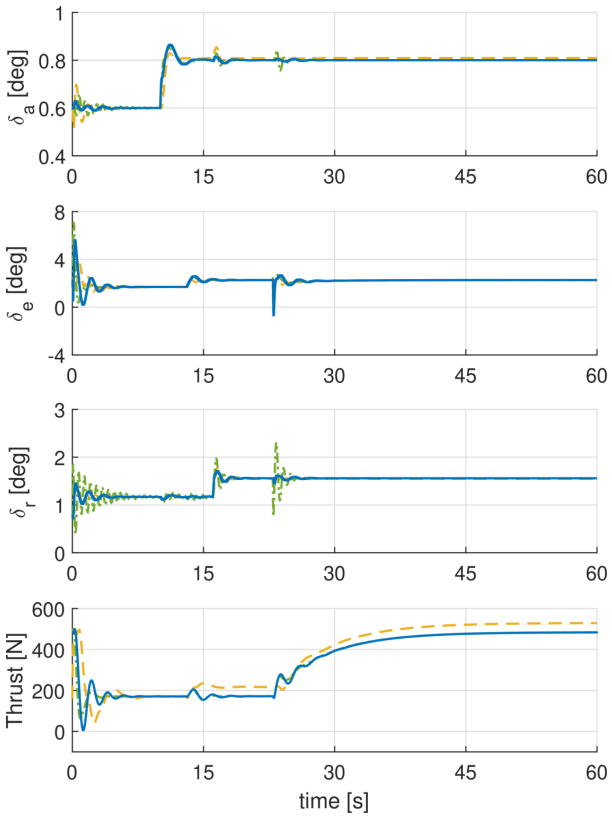

Fig. 4. Control inputs under 25% loss-of-control.

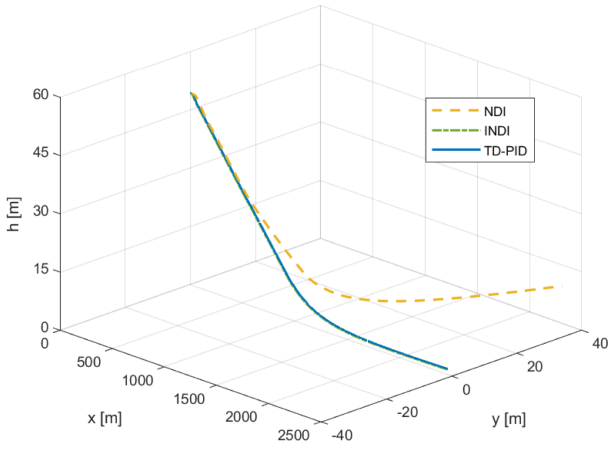

Fig. 5. Landing performance under 25% loss-of-control.

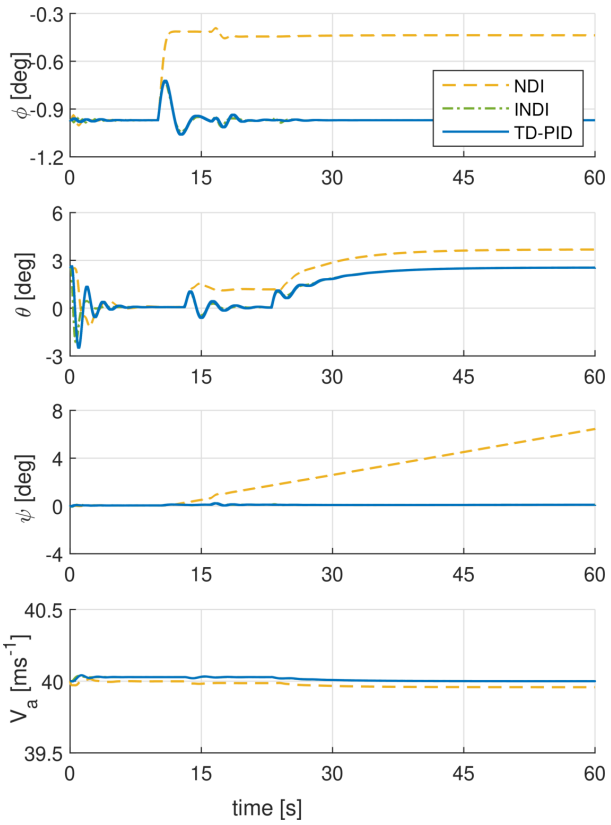

Fig. 6. Attitude and Airspeed response under 50% loss-of-control.

relationship between INDI and TDC as $T_{D_i} = 0.143$ and $T_{I_i} = 0.28$. The proportional gain $\breve{\boldsymbol{K}}$ is tuned analytically based on the nominal values of the effector blending moments $\breve{\boldsymbol{\mathcal{B}}}$ of the aircraft, as used in the INDI controller. A separate control loop for airspeed hold is designed using a proportional-integral thrust control. The sampling frequency used in the simulation is $f_s = 100Hz$ and the corresponding sampling time is taken as $\tau = 0.01s$. For simplicity, the delay time and the sampling time are considered to be the same.

Actuator loss-of-control is introduced in form of degradation in control effectiveness in the aileron, the elevator and the rudder in a successive manner at 10s, 13s and 16s, respectively. Under 25% loss-of-control, the aircraft attitude

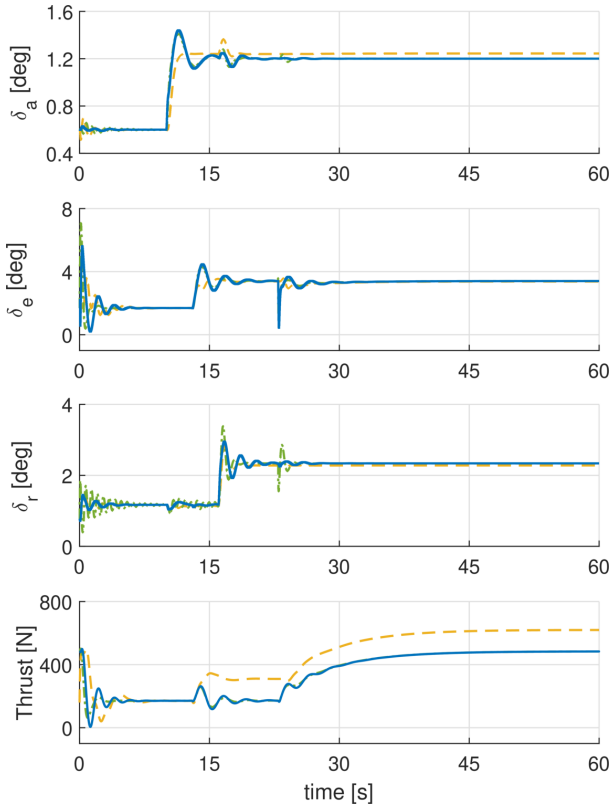

Fig. 7. Control inputs under 50% loss-of-control.

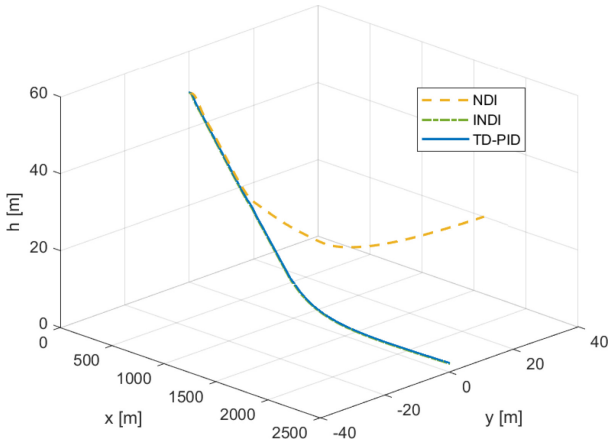

Fig. 8. Landing performance under 50% loss-of-control.

Table 3. Initial Trim Conditions

V_∞	40 ms^{-1}	ϕ	$-0.98°$	p	$0.0°s^{-1}$	δ_a	$0.60°$
α	$2.58°$	θ	$2.58°$	q	$0.0°s^{-1}$	δ_e	$1.69°$
β	$0.00°$	ψ	$-0.05°$	r	$0.0°s^{-1}$	δ_a	$1.17°$

and airspeed responses and the control input time histories are presented in Figs. 3 and 4, respectively, and the landing performance is illustrated in Fig. 5. It can be observed that the TD-PID exhibits similar robustness characteristics to the INDI controller, whereas the NDI controller suffers a performance degradation under actuator loss-of-control. Figs. 6, 7 and 8 illustrate that the TD-PID is once again consistent and delivers a performance that is in par with the INDI in coping up with the loss-of-control condition, while NDI suffers more performance degradation. The

performance metrics of all the controllers in terms of the root mean square tracking error is summarised in Table 4.

Table 4. Controller Performance Metrics.

Control	LOC [%]	$rms(e_\phi)$ [deg]	$\text{rms}(e_\theta)$ [deg]	$\text{rms}(e_\psi)$ [deg]	$\text{rms}(e_h)$ [m]
NDI	[25]	0.156	0.333	0.046	6.565
	[50]	0.468	0.974	0.143	18.710
INDI	[25]	0.019	0.202	0.006	0.642
	[50]	0.029	0.217	0.013	0.827
TD-PID	[25]	0.011	0.278	0.005	0.648
	[50]	0.032	0.294	0.015	0.819

In an overall sense, a PID controller designed within a time-delay framework and gain tuning based on INDI approach can exhibit better robustness characteristics and can be regarded as an effective methodology for robust fault-tolerant flight control.

5. CONCLUSION

A time-delay based PID control scheme was demonstrated for automatic landing of the Hansa-3 aircraft under successive actuator faults. The framework for PID control design for automatic landing in terms of aircraft attitude control was established theoretically for the input-output mapping in second-order controller canonical form. The PID gains are tuned based on incremental nonlinear dynamic inversion. Simulation results suggest that the TD-PID controller exhibits similar robustness characteristics to INDI controller under off-nominal flight conditions, thus making it an effective means to implement fault-tolerant flight control. The proposed control approach can be extended to cope up with model uncertainties like structural damage and multiple actuator impairments combined with external disturbances during auto-landing phase.

REFERENCES

Acquatella, P., Falkena, W., van Kampen, E.J., and Chu, Q.P. (2012). Robust nonlinear spacecraft attitude control using incremental nonlinear dynamic inversion. In *AIAA Guidance, Navigation, and Control Conference*, 4623.

Acquatella, P., van Ekeren, W., and Chu, Q.P. (2017). Pi(d) tuning for flight control systems via incremental nonlinear dynamic inversion. *IFAC-PapersOnLine*, 50(1), 8175–8180.

Chang, P.H. and Jung, J.H. (2008). A systematic method for gain selection of robust pid control for nonlinear plants of second-order controller canonical form. *IEEE Transactions on Control Systems Technology*, 17(2), 473–483.

Choi, H.S., Lee, S., Lee, J., Kim, E.T., and Shim, H. (2010). Aircraft longitudinal auto-landing guidance law using time delay control scheme. *Transactions of the Japan Society for Aeronautical and Space Sciences*, 53(181), 207–214.

Jung, J., Chang, P., and Stefanov, D. (2011). Discretisation method and stability criteria for non-linear systems under discrete-time time delay control. *IET control theory & applications*, 5(11), 1264–1276.

Kim, K.S., Lee, K.J., and Kim, Y. (2003). Reconfigurable flight control system design using direct adaptive method. *Journal of guidance, control, and dynamics*, 26(4), 543–550.

Kumar, A. and Ghosh, A.K. (2018). Data-driven method based aerodynamic parameter estimation from flight data. In *2018 AIAA Atmospheric Flight Mechanics Conference*, 0768.

Lee, J., Choi, H.S., Lee, S., Kim, E.T., and Shin, D. (2012). Time delay fault tolerant controller for actuator failures during aircraft autolanding. *Transactions of the Japan Society for Aeronautical and Space Sciences*, 55(3), 175–182.

Lombaerts, T., Chu, P., Mulder, J.A.B., and Stroosma, O. (2011). Fault tolerant flight control, a physical model approach. *Advances in Flight Control Systems*.

Marquez-Martinez, L. and Moog, C.H. (2004). Input-output feedback linearization of time-delay systems. *IEEE Transactions on Automatic Control*, 49(5), 781–785.

Peyada, N. and Ghosh, A. (2009). Aircraft parameter estimation using neural network based algorithm. In *AIAA atmospheric flight mechanics conference*, 5941.

Reddy, S.B. (2020a). New analysis/design of generalized discrete pi controller via discrete time delay control for nonlinear systems. In *Dynamic Systems and Control Conference*, volume 84270, V001T04A003. American Society of Mechanical Engineers.

Reddy, S.B. (2020b). New stability analysis and design of discrete time delay control for nonaffine nonlinear systems. In *Dynamic Systems and Control Conference*, volume 84270, V001T04A002. American Society of Mechanical Engineers.

Roy, S., Kar, I.N., Lee, J., and Jin, M. (2017a). Adaptive-robust time-delay control for a class of uncertain euler–lagrange systems. *IEEE Transactions on Industrial Electronics*, 64(9), 7109–7119.

Roy, S., Roy, S.B., and Kar, I.N. (2017b). Adaptive robust control of euler–lagrange systems with linearly parametrizable uncertainty bound. *IEEE Transactions on Control Systems Technology*, 26(5), 1842–1850.

Sieberling, S., Chu, Q., and Mulder, J. (2010). Robust flight control using incremental nonlinear dynamic inversion and angular acceleration prediction. *Journal of guidance, control, and dynamics*, 33(6), 1732–1742.

Simplício, P., Pavel, M., Van Kampen, E., and Chu, Q. (2013). An acceleration measurements-based approach for helicopter nonlinear flight control using incremental nonlinear dynamic inversion. *Control Engineering Practice*, 21(8), 1065–1077.

Smeur, E.J., Chu, Q., and De Croon, G.C. (2016). Adaptive incremental nonlinear dynamic inversion for attitude control of micro air vehicles. *Journal of Guidance, Control, and Dynamics*, 39(3), 450–461.

Youcef-Toumi, K. and Wu, S.T. (1992). Input/output linearization using time delay control.

Zhang, Y. and Jiang, J. (2008). Bibliographical review on reconfigurable fault-tolerant control systems. *Annual reviews in control*, 32(2), 229–252.